CONCEPTION OF COVALENTLY REVERSIBLE SEMI-PEPTIDIC INHIBITORS OF TMPRSS2 FOR SARS-COV-2 TREATMENT

Sára Ferková, Antoine Désilets, Matthieu Lepage, Kevin Assouvie, Gabriel Lemieux, Ulrike Froehlich, Jules Vastra, Alice Gravel-Trudeau, Philippe Sarret, Richard Leduc and Pierre-Luc Boudreault

Department of Pharmacology and Physiology, Faculty of Medicine and Health Sciences, Pharmacology Institute of Sherbrooke (IPS), Université de Sherbrooke, QC, Canada

INTRODUCTION

Since 2019, SARS-CoV-2 has undergone extensive genomic mutations, leading to resistance to various COVID-19 treatments. The development of selective, host-directed therapeutics that benefit from virus-host tropism enables a large-scale prevention and treatment. In this study, we present our drug discovery process targeting the type II transmembrane serine protease (TMPRSS2), which has been validated as a therapeutic target due to its role in proteolytical cleavage of the SARS-CoV-2 Spike (S) protein, thereby mediating host cell infection.

In our previous work[1], we identified **N-0385**, a highly potent covalent-reversible TMPRSS2 inhibitor, as a lead candidate. This inhibitor contains a ketobenzothiazole-based serine trap for covalent binding. However, during preclinical evaluations for intranasal administration, **N-0385** exhibited unfavorable pharmacokinetic properties, including excessively high bioavailability (99%), resulting in significant systemic exposure that limited progress in pre-clinical and clinical studies.

The objective was to overcome the high lung permeability and the lack of TMPRSS2 selectivity over Factor Xa. By targeting the well-conserved catalytic triad and the S1 and S1' pockets, we expected selectivity and permeability modifications to depend on the unexplored P3-substitution. Therefore, we first designed a small library of peptidomimetic compounds with P3 site modifications, achieved by substituting with proteinogenic amino acids. We then screened for *in vitro* TMPRSS2 inhibition and SARS-CoV-2 antiviral activity. The rationally designed library enabled us to identify pharmacophoric features for Factor Xa selectivity through LowModeMD (Molecular Dynamics + Conformational Search) simulations and covalent docking, while also reducing permeability in a bronchial epithelial cell permeability model.

1 Shapira T. et al., Nature (**2022**)

TARGET IDENTIFICATION and HIT SELECTION

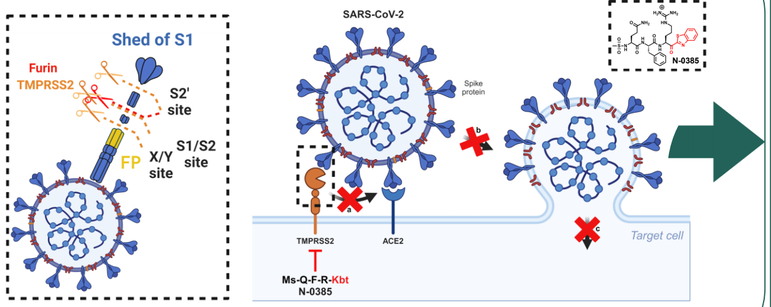

Figure 1. Schematic representation of TMPRSS2 inhibition by **N-0385** by blocking TMPRSS2-dependent Spike cleavage **(a)**, subsequent fusion of the target cell and viral membrane **(b)**, and release of viral genome **(c)**.

CONCLUSION

As expected, all compounds exhibited excellent inhibitory activity against TMPRSS2 (Ki < 2 nM) and efficiently reduced viral infection in the pseudovirus assay. Exceptionally, compound **9**, containing Asp in position P3, demonstrated a 2-fold increase in TMPRSS2 sub-nanomolar inhibitory potency (Ki = 0.13 ± 0.03 nM) and showed superior selectivity against other proteases (Factor Xa, matriptase, TMPRSS6, thrombin, and furin). In the air-liquid interface (ALI) model of pulmonary epithelium, compound **9** displayed a 1.5-fold reduction in permeability compared to **N-0385**, with sustained stability in lung (11 h) and plasma (13 h), suggesting potential for further exploration via intranasal administration.

Further *in vivo* pharmacokinetic studies are underway, which may lead to preclinical and clinical trials.

LEAD OPTIMIZATION

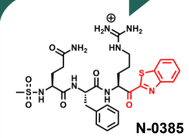

IN VIVO PHARMACOKINETICS

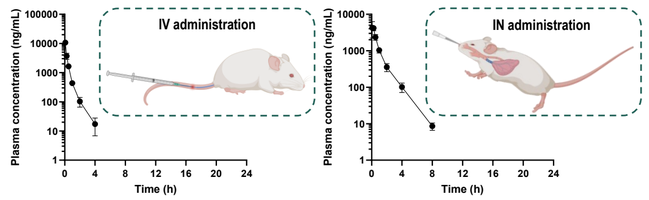

Administration (5 mg/kg)	$AUC_{0\text{-}last}$ (ng*h/mL)	$AUC_{0\text{-}\infty}$ (ng*h/mL)	C_{max} (ng/mL)	T_{max} (h)	$t_{1/2}$ (h)
Intravenous (IV)	3690 ± 47	3707 ± 53	18315 ± 2886	-	0.6 ± 0.1
Intranasal (IN)	3621 ± 746	3674 ± 795	4783 ± 1184	0.139 ± 0.096	1.05 ± 0.16

Figure 2. Pharmacokinetic parameters of **N-0385**. Data points represent average ± SD from three independent experiments and plotted using GraphPad Prism 9.

PRE-CLINICAL TRIALS

REVISITING

REDESIGN OF INHIBITORS

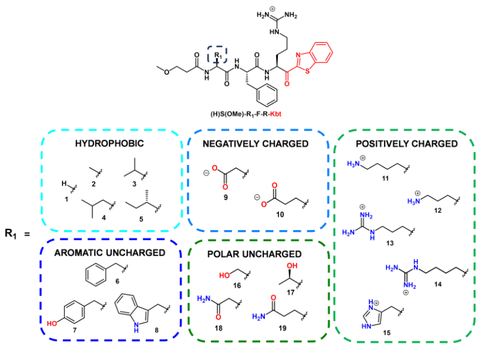

Figure 3. Structural modifications of ketobenzotiazole-based compound with color-coded classification of substituted amino acids based on side-chain (R_1) characteristics.

IN VITRO PHARMACOKINETICS

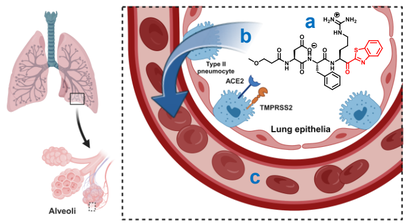

Figure 7. Schematic representation of the transfer of compound **9** from the lung to the blood, with a focus on the lung compartment (**a**), drug absorption process (**b**), and systemic exposure (**c**).

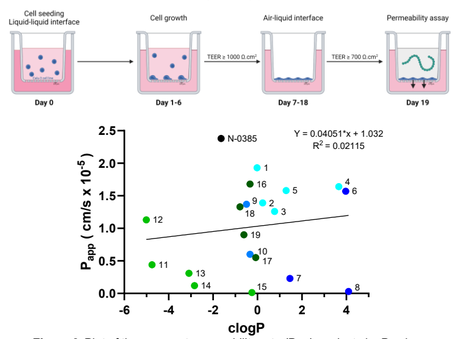

Figure 8. Plot of the apparent permeability rate (P_{app}) against clogP values experimentally determined in the bronchial epithelial cell permeability model.

TMPRSS2 SELECTIVITY

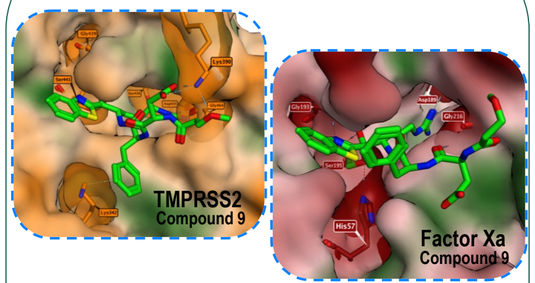

Figure 5. Binding mode of **9** in the TMPRSS2 and Factor Xa active site.
The nature of each surface is color-coded, ranging from hydrophilic (orange, red), neutral (white) to lipophilic (green). Non-covalent interactions are depicted as dashed lines with a strength bar using Molecular Operating Environment software (MOE).

K_i (nM ± SD)	Compound 9	N-0385
TMPRSS2	0.13 ± 0.03	0.28 ± 0.03
Factor Xa	92.6 ± 17.2	21.1 ± 5.5
Matriptase	13.97 ± 0.65	2.6 ± 0.4
TMPRSS6	2.86 ± 0.14	0.75 ± 0.05
Thrombin	> 10000	9271 ± 647
Furin	> 10000	> 10000

Figure 6. Enzyme inhibition constants (K_i) for selected proteases.

IN VITRO STRUCTURE-ACTIVITY RELATIONSHIP

Compound	Ki TMPRSS2 (nM ± SD)
1	0.33 ± 0.09
2	0.38 ± 0.11
3	0.41 ± 0.13
4	0.36 ± 0.10
5	0.60 ± 0.16
6	0.29 ± 0.06
7	0.37 ± 0.04
8	0.39 ± 0.05
9	**0.13 ± 0.03**
10	**0.14 ± 0.02**
11	0.70 ± 0.07
12	0.39 ± 0.05
13	**0.15 ± 0.0003**
14	**0.16 ± 0.01**
15	0.85 ± 0.05
16	0.53 ± 0.03
17	0.44 ± 0.12
18	1.55 ± 0.17
19	0.34 ± 0.07
N-0385	**0.28 ± 0.03**

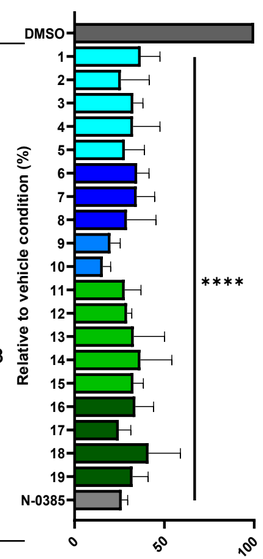

Figure 4. Enzyme inhibition constants (K_i) for TMPRSS2 and SARS-CoV-2 pseudoviral infection inhibition by compounds **1-19** and **N-0385.**

INSTITUT DE PHARMACOLOGIE DE SHERBROOKE UdS

Université de Sherbrooke

CENTRE DE RECHERCHE CHUS

NSERC CRSNG

IRSC CIHR Instituts de recherche en santé du Canada / Canadian Institutes of Health Research

BOUDREAULT MEDICINAL CHEMISTRY LAB